Supplementary Materials to Blind Image Deblurring with Local Maximum Gradient Prior

Liang Chen Faming Fang* Tingting Wang Guixu Zhang
Shanghai Key Laboratory of Multidimensional Information Processing, and
Department of Computer Science and Technology, East China Normal University, Shanghai, China

In this supplementary file, we provide,
1. Details of the algorithm provided in the paper.
2. Extension to non-uniform deblurring
3. More examples of our model with and without LMG prior.
4. More comparison results with other state-of-the-art methods.

1. Details of the algorithm

As demonstrated in the paper. Our model with LMG prior is,

$$\min_{I,K} \|I \otimes K - B\|^2 + \beta\|2 - LMG(I)\|_1 + \gamma\|\nabla I\|_0 + \tau\|K\|^2. \tag{1}$$

We split it into 2 sub problems referring to I and K, respectively. AS shown in bellow,

$$\begin{cases} \min_{I} \|I \otimes K - B\|^2 + \beta\|2 - LMG(I)\|_1 + \gamma\|\nabla I\|_0, & (2)\\ \min_{K} \|I \otimes K - B\|^2 + \tau\|K\|^2. & (3)\end{cases}$$

We now optimize Eq. (2) and (3) independently with another fixed.

1.1. Estimate latent image

We introduce new substitution variable $u \to 2 - LMG(I)$ and $g \to \nabla I$, Eq. (2) can be rewritten as,

$$\min_{I,u,g} \|I \otimes K - B\|^2 + \beta\|u\|_1 + \gamma\|g\|_0 + \alpha_1\|2 - LMG(I) - u\|^2 + \alpha_2\|\nabla I - g\|^2, \tag{4}$$

where α_1 and α_2 are the penalty parameters. We can solve Eq. (4) by optimizing I, u, g alternatively while fixing others.

Update I. As mentioned in Section 3 of the paper, the LMG operation can be seen as a matrix applied to the vector form image, i.e., $LMG(I) = \mathbf{G}\mathbf{I}$, where $\mathbf{I}$ denotes the vector form I. Thus, the problem referring to I can be written as,

$$\min_{\mathbf{I}} \|\mathbf{K}\mathbf{I} - \mathbf{B}\|^2 + \alpha_1\|2 - \mathbf{G}\mathbf{I} - \mathbf{u}\|^2 + \alpha_2\|\nabla\mathbf{I} - \mathbf{g}\|^2, \tag{5}$$

here we use $\mathbf{K}$ to denote toeplitz form of blur kernel K, $\mathbf{B}$, $\mathbf{u}$ and $\mathbf{g}$ to denote vector form of B, u, g, respectively. Eq. (5) is quadric problem refer to $\mathbf{I}$. Taking derivative of $\mathbf{I}$ and set it to 0, we have,

$$(\mathbf{K}^T\mathbf{K} + \alpha_1\mathbf{G}^T\mathbf{G} + \alpha_2\nabla^T\nabla)\mathbf{I} = \mathbf{K}^T\mathbf{B} + \alpha_1\mathbf{G}^T(2 - \mathbf{u}) + \alpha_2\nabla^T\mathbf{g}. \tag{6}$$

We can solve it with a conjugate gradient method.However, the size of $\mathbf{G}$ will requires tremendous time to convergence. For example, it takes about 878.16 second to deblur a 255×255 image, while our proposed method takes about 65.20 second to deblur the same object. Thus, we introduce another auxiliary variable $\mathbf{q}$ for $\mathbf{I}$ in the second term of Eq. (5) as a trade off between speed and accuracy. We have,

$$\min_{\mathbf{I},\mathbf{q}} \|\mathbf{K}\mathbf{I} - \mathbf{B}\|^2 + \alpha_1\|2 - \mathbf{G}\mathbf{q} - \mathbf{u}\|^2 + \alpha_2\|\nabla\mathbf{I} - \mathbf{g}\|^2 + \alpha_3\|\mathbf{I} - \mathbf{q}\|^2, \tag{7}$$

where α_3 is a positive penalty parameter. We can solve Eq. (7) by updating $\mathbf{I}$ and $\mathbf{q}$ in an alternative manner, which is given by,

$$\begin{cases} \min_{\mathbf{I}} \|\mathbf{KI}-\mathbf{B}\|^2 + \alpha_2\|\nabla\mathbf{I}-\mathbf{g}\|^2 + \alpha_3\|\mathbf{I}-\mathbf{q}\|^2, & (8) \\ \min_{\mathbf{q}} \alpha_1\|2-\mathbf{Gq}-\mathbf{u}\|^2 + \alpha_3\|\mathbf{I}-\mathbf{q}\|^2. & (9) \end{cases}$$

Taking the derivative of the variables and set them to zeroes, we can easily obtain the optimal solution,

$$\begin{cases} \mathbf{I} = \mathcal{F}^{-1}\dfrac{\overline{\mathcal{F}(\mathbf{K})}\mathcal{F}(\mathbf{B}) + \alpha_2\overline{\mathcal{F}(\nabla)}\mathcal{F}(\mathbf{g}) + \alpha_3\mathcal{F}(\mathbf{q})}{\overline{\mathcal{F}(\mathbf{K})}\mathcal{F}(\mathbf{K}) + \alpha_2\overline{\mathcal{F}(\nabla)}\mathcal{F}(\nabla) + \alpha_3}, & (10) \\ \mathbf{q} = \dfrac{\alpha_1\mathbf{G}^T(2-\mathbf{u}) + \alpha_3\mathbf{I}}{\mathbf{G}^T\mathbf{G} + \alpha_3}. & (11) \end{cases}$$

where $\mathcal{F}(\cdot)$ and $\overline{\mathcal{F}(\cdot)}$ denote FFT and its conjugate, and $\mathcal{F}^{-1}(\cdot)$ represent inverse FFT.

Update u. With given I, the problem refer to u is,

$$\min_{\mathbf{u}} \beta\|\mathbf{u}\|_1 + \alpha_1\|2-\mathbf{GI}-\mathbf{u}\|^2. \tag{12}$$

It is an one-dimension shrinkage, and the solution can be written as,

$$\mathbf{u} = sign(2-\mathbf{GI})\cdot\max(|2-\mathbf{GI}| - \frac{\beta}{2\alpha_1}, 0).$$

Update g. With the other two variable fixed, problem refer to g can be written as,

$$\min_{\mathbf{g}} \lambda\|\mathbf{g}\|_0 + \alpha_2\|\nabla\mathbf{I}-\mathbf{g}\|^2. \tag{13}$$

The solution is,

$$\mathbf{u} = sign(2-\mathbf{GI})\cdot\max(|2-\mathbf{GI}| - \frac{\beta}{2\alpha_1}, 0).$$

The overall procedure to estimate latent image is summarized in Algorithm 1.

Algorithm 1: Estimate latent image (refer to Eq. (10) in the paper)

Input: Blurry image B, blur kernel K
$I \leftarrow B$. $\alpha_1 \leftarrow \alpha_{1init}$
while $\alpha_1 < \alpha_{1max}$ **do**
  Solve for matrix **G**.
  Solve u according to Eq. ((12)).
  $\alpha_2 \leftarrow \alpha_{2init}$.
  while $\alpha_2 < \alpha_{2max}$ **do**
    Solve for g according to Eq. ((13)).
    $\alpha_3 \leftarrow \alpha_{3init}$.
    while $\alpha_3 < \alpha_{3max}$ **do**
      Solve for q according to Eq. ((9)).
      Solve for I according to Eq. ((8)).
      $\alpha_3 \leftarrow 2\alpha_3$
    end
    $\alpha_2 \leftarrow 2\alpha_2$
  end
  $\alpha_1 \leftarrow 2\alpha_1$
end
Output: Blur kernel K. Intermediate latent image I.

Algorithm 2: Blur kernel estimation with LMG prior algorithm

Input: Blurry image B

Initialize K from the coarser level.

while *iter = 1:maxiter* **do**

  Update I with Algorithm 1.

  Update K with Eq. (14).

end

Output: Blur kernel K. Intermediate latent image I.

1.2. Estimate kernel

As demonstrated in the paper, we adopt the strategy from [1] for the kernel estimation step. Eq. (3) is redefined as,

$$\min_{K} \|\nabla I \otimes K - \nabla B\|^2 + \tau \|K\|^2. \tag{14}$$

We can solve it with FFT directly. The answer is given by,

$$K = \frac{\overline{\mathcal{F}(\nabla I)}\mathcal{F}(\nabla B)}{\overline{\mathcal{F}(\nabla I)}\mathcal{F}(\nabla I) + \tau}.$$

The overall algorithm for the deblurring process is summarized in Algorithm 2.

2. Extension to Non-uniform Deblurring

Our model can be easily extended to non-uniform deblurring where the blur kernel in a image is spatial-variant. Based on the geometric model of camera motion [12, 13], the blurry image can be modeled as a weighted sum of latent image under geometry transformations,

$$\mathbf{B} = \sum_{t} k_t \mathbf{h}_t \mathbf{I} + \mathbf{n}, \tag{15}$$

where $\mathbf{B}, \mathbf{I}$ and $\mathbf{n}$ denote blurry image, latent image and noise in vector form, respectively; t is the index of camera pose samples, and k_t is the corresponding weight; $\mathbf{H}_t$ denotes a homography matrix. Similar to [13], we reformulate Eq. (15) as,

$$\mathbf{B} = \mathbf{HI} + \mathbf{n} = \mathbf{zk} + \mathbf{n}, \tag{16}$$

where $\mathbf{H} = \sum_t k_t \mathbf{h}_t$, $\mathbf{z} = [\mathbf{h}_1\mathbf{I}, \mathbf{h}_1\mathbf{I}, ..., \mathbf{h}_t\mathbf{I}]$, and $\mathbf{k} = [k_1, k_2, ..., k_t]^T$. Based on Eq. (16), the non-uniform deblurring problem is solved by alternatively minimizing,

$$\begin{cases} \min\limits_{\mathbf{I}} \|\mathbf{HI} - \mathbf{B}\|_2^2 + \beta \|2 - LMG(\mathbf{I})\|_1 + \gamma \|\nabla \mathbf{I}\|_0, & (17) \\ \min\limits_{\mathbf{k}} \|\mathbf{zk} - \mathbf{B}\|_2^2 + \tau \|\mathbf{k}\|_2^2. & (18) \end{cases}$$

The updating details are similar to the uniform deblurring case, and latent image $\mathbf{I}$ and the weight $\mathbf{k}$ are estimated by the fast forward approximation [4]. Example of our non-uniform deblurring effect is shown in Section 4 in this supplementary material.

3. Deblurring examples without LMG prior

We have analysed the effectiveness of the LMG prior in the paper in section 5.1. Experimental results demonstrates our model with LMG is more effective. In this section we will provide more examples to intuitively illustrates the difference between with and without LMG prior.

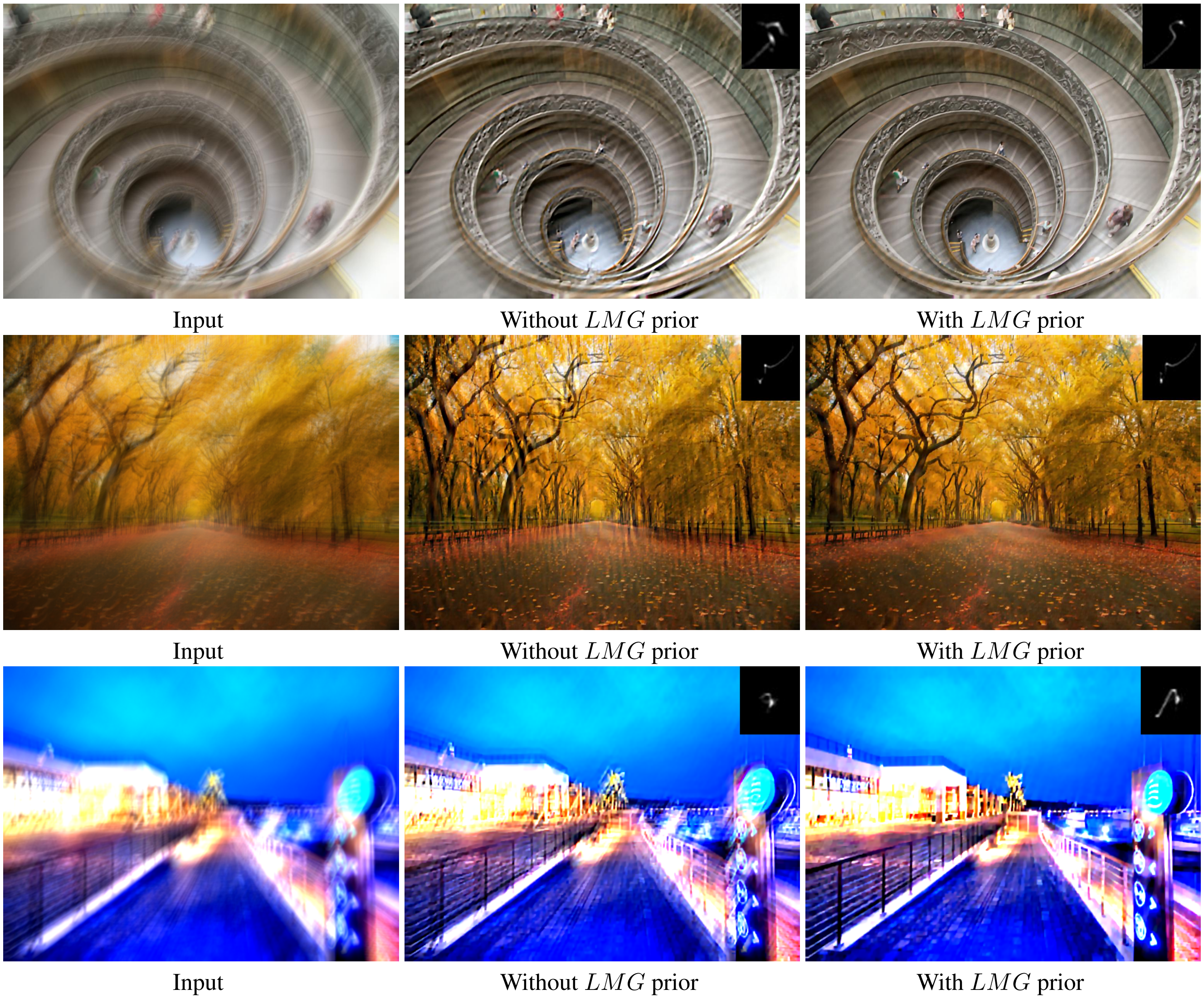

Figure 1. Three challenging examples from dataset [7]. Our model without LMG prior is less effective, while our model with LMG prior generates more visual pleasing results. Demonstrating the effectiveness of the proposed LMG prior. Both theoretical and empirical analysis demonstrates LMG prior can help restore blurry image.

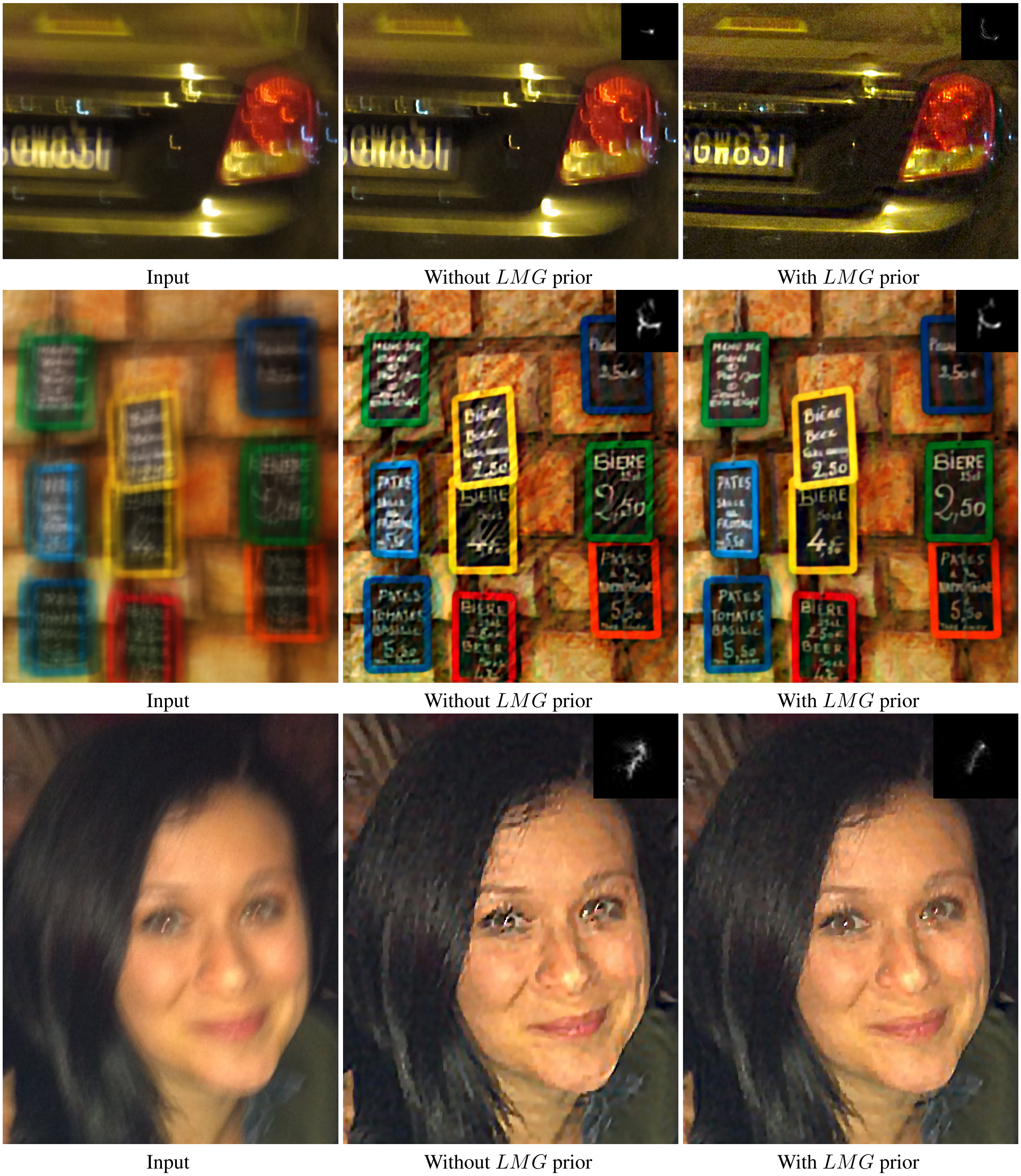

Figure 2. Three examples on given specific occasions (noise, face and text). We use the same non-blind deconvolution method from [2] Our model without LMG prior is less effective, while our model with LMG prior generates more visual pleasing results. Demonstrating the effectiveness of the proposed LMG prior. Both theoretical and empirical analysis demonstrates LMG prior can help restore blurry image.

4. Comparison with state-of-the-art methods

We have conduct experiments on several datasets and compare the results with state-of-the-art methods. As illustrated in section 4 of the paper, our methods generate better overall results among these methods. In this section, we will provide more examples to intuitively express the advantage of LMG prior. Comparison objects are deconved by same non-blind deconvolution methods after kernels are acquired.

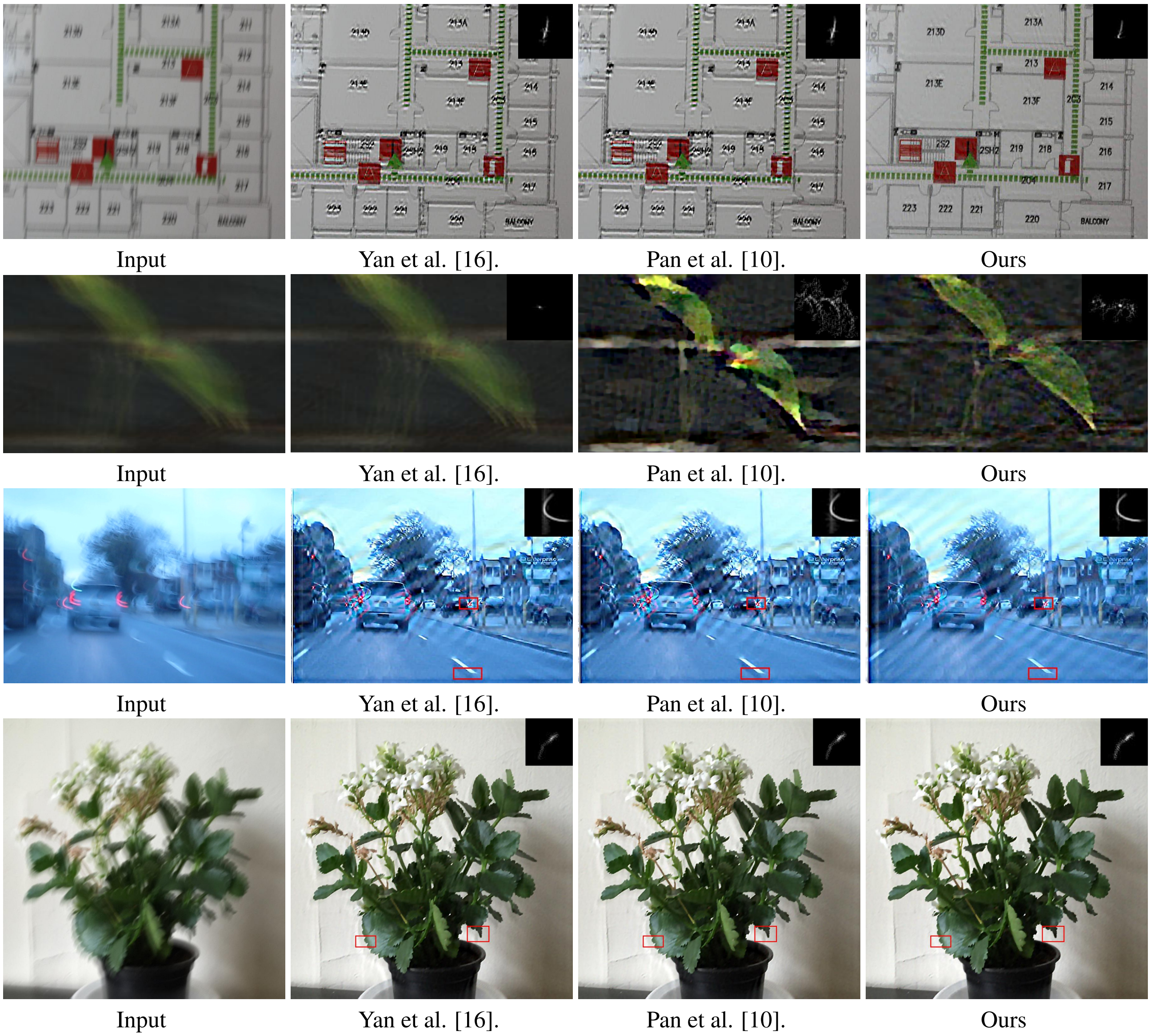

Figure 3. Four examples on real-world blur images. Our method generates more visual pleasing results that the state-of-the-art L_0 based methods (Details contained in red boxes are best viewed on high-resolution display with zoom in).

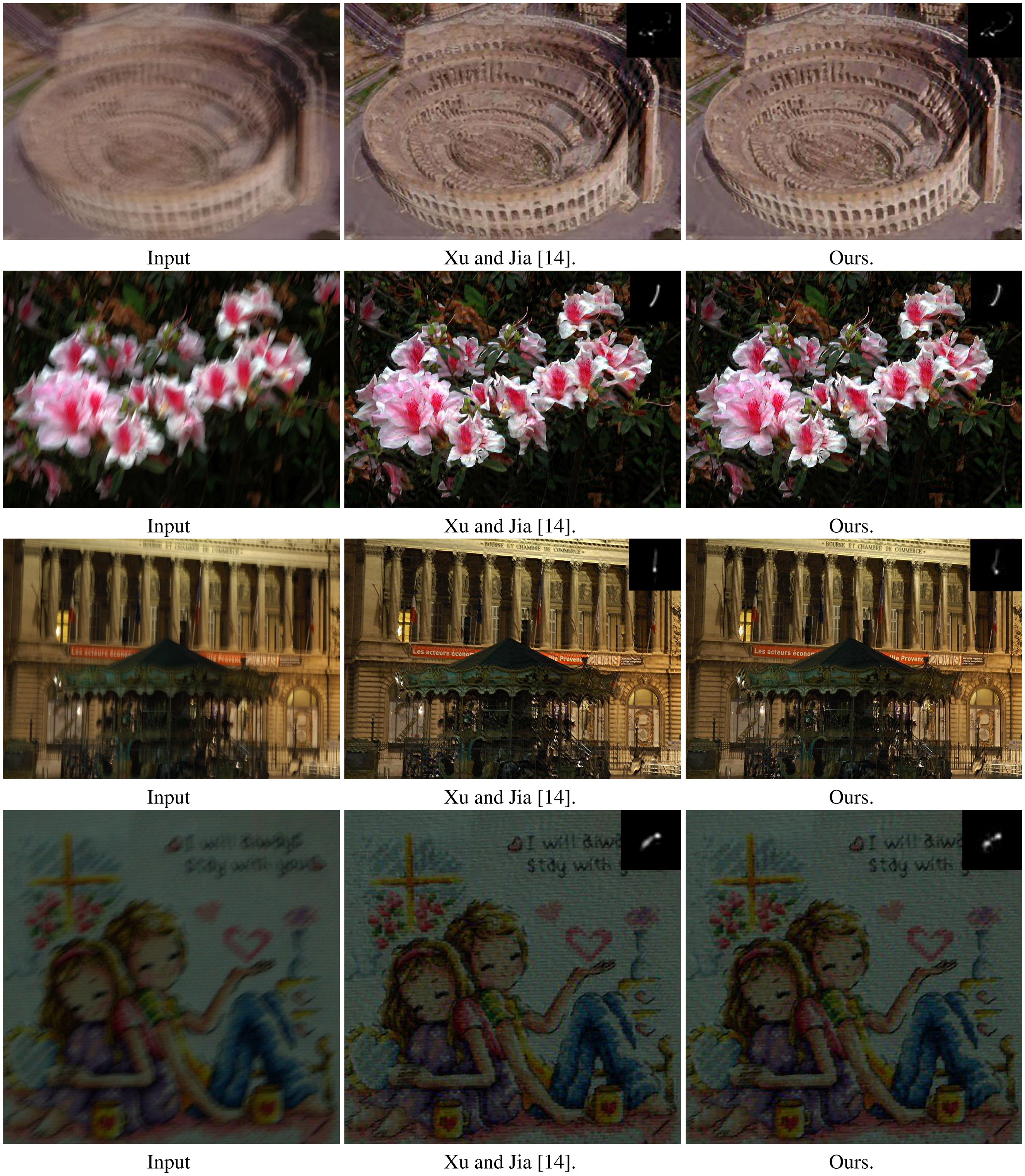

Figure 4. Natural image deblurring examples from [14]. Our method generates visually comparable or even better deblurring results compared to [14].

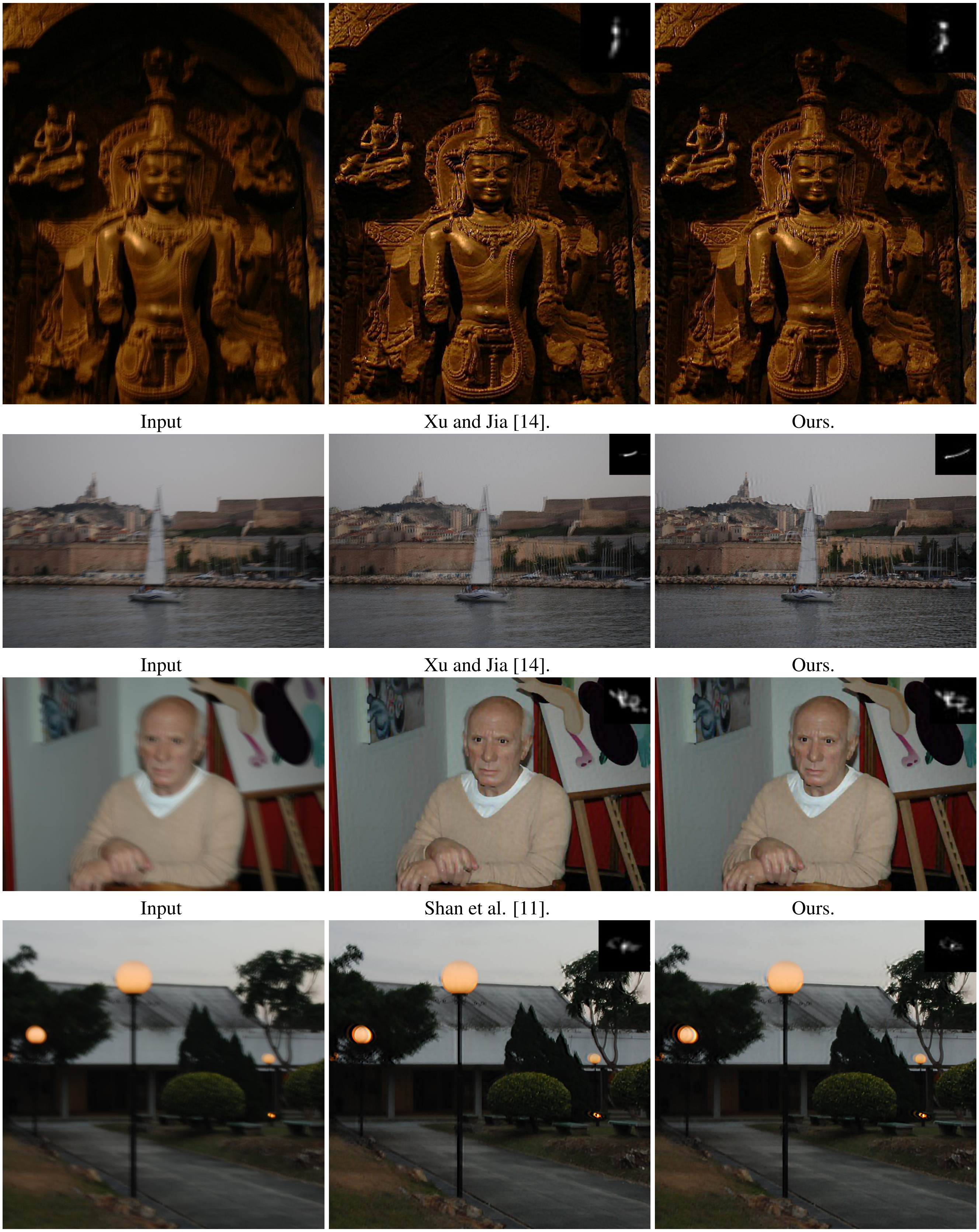

Input | Xu and Jia [14]. | Ours.

Input | Xu and Jia [14]. | Ours.

Input | Shan et al. [11]. | Ours.

Input | Shan et al. [11]. | Ours.

Figure 5. Deblurring results using given examples. Our method generates visually comparable or even better results.

Input | Cho and Lee[1]. | Ours.

Input | Cho and Lee[1]. | Ours.

Input | Fergus et al. [3]. | Ours.

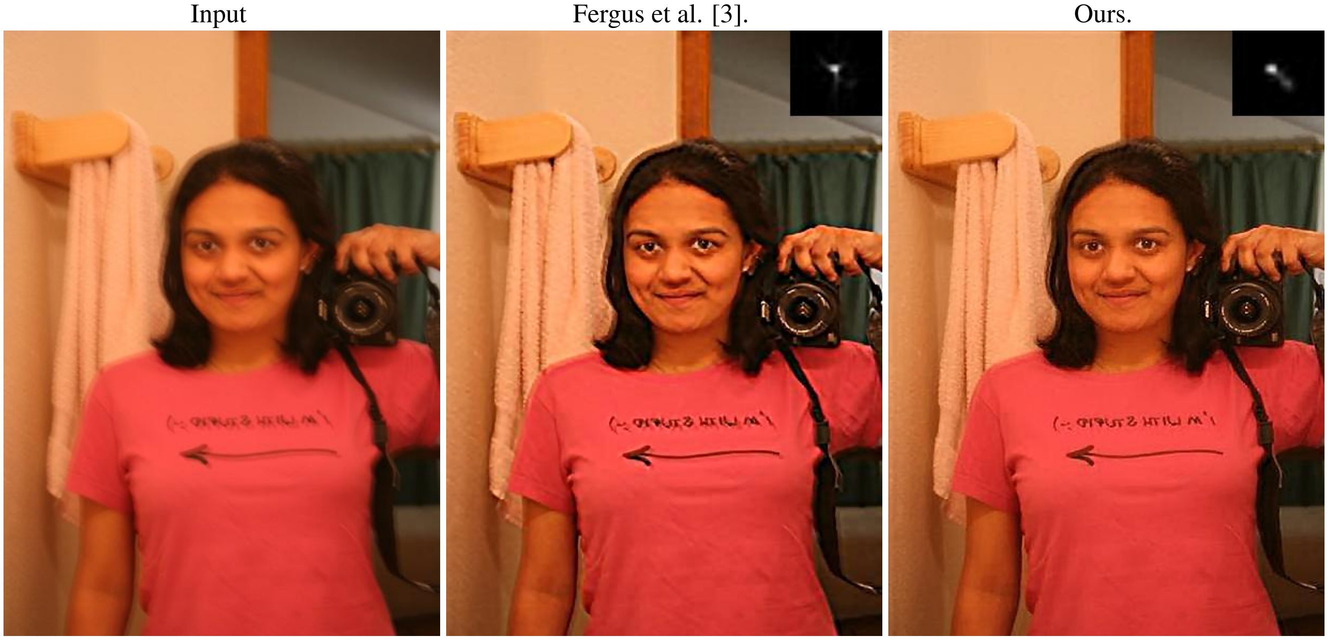

Input | Krishnan et al. [6]. | Ours.

Figure 6. Deblurring results using given examples. Our method generates visually comparable or even better results.

Figure 7. Deblurring text blur images. Our method generates visually comparable or even better results specially designed for text deblurring method [9].

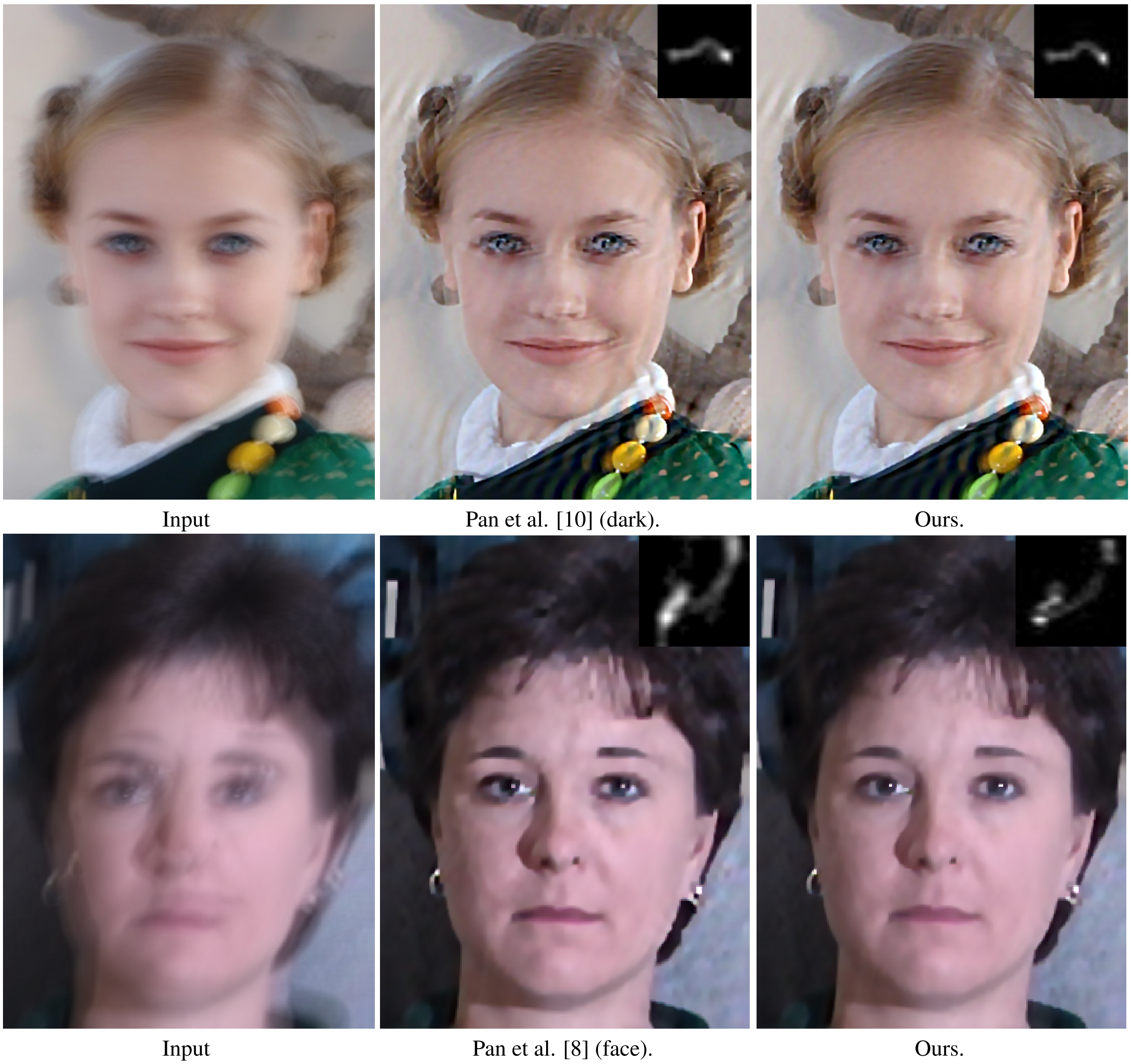

Figure 8. Deblurring face blur images. Our method generates visually comparable or even better results than state-of-the-art methods.

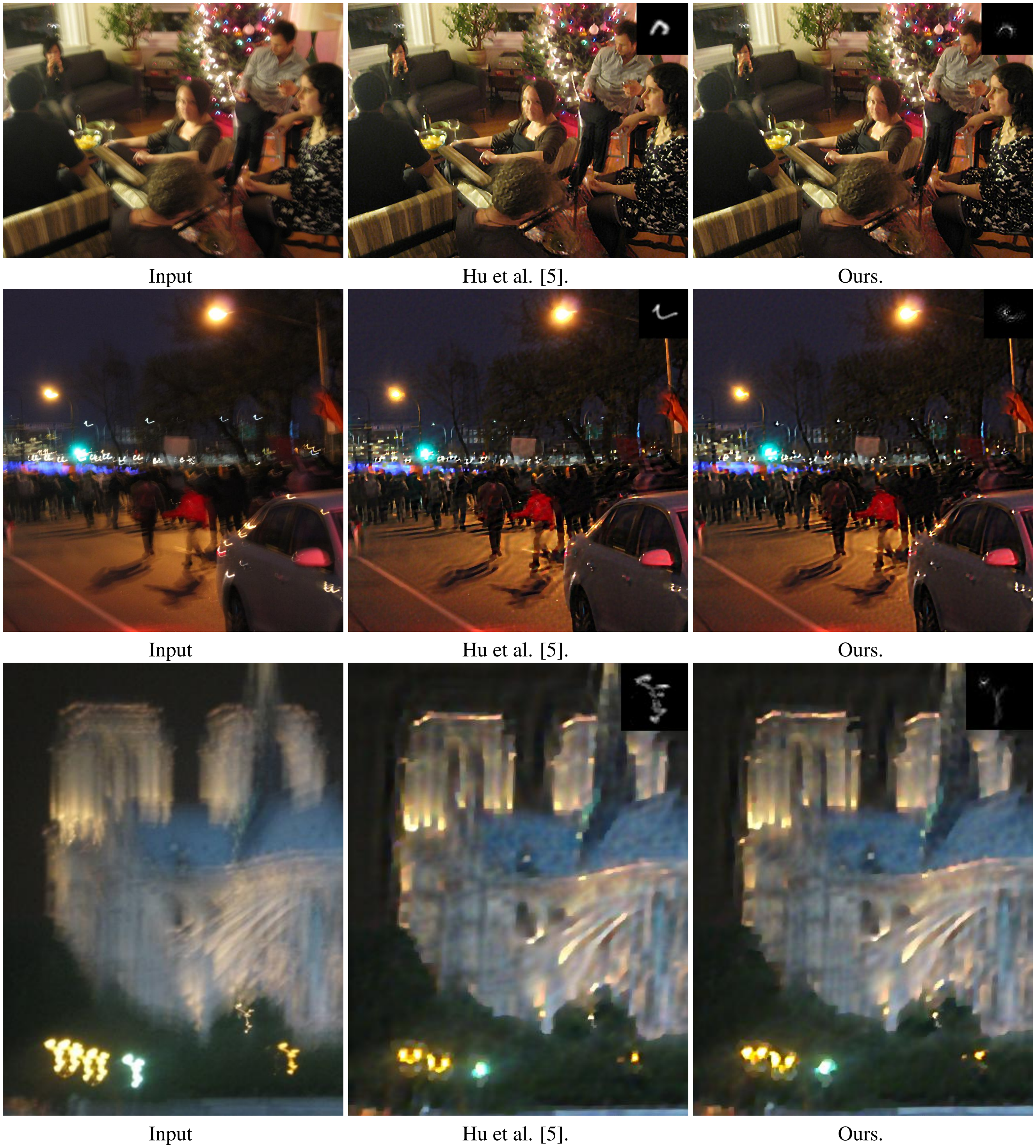

Figure 9. Deblurring low-illumination blur images. Our method generates visually comparable or even better results than specially designed method[5].

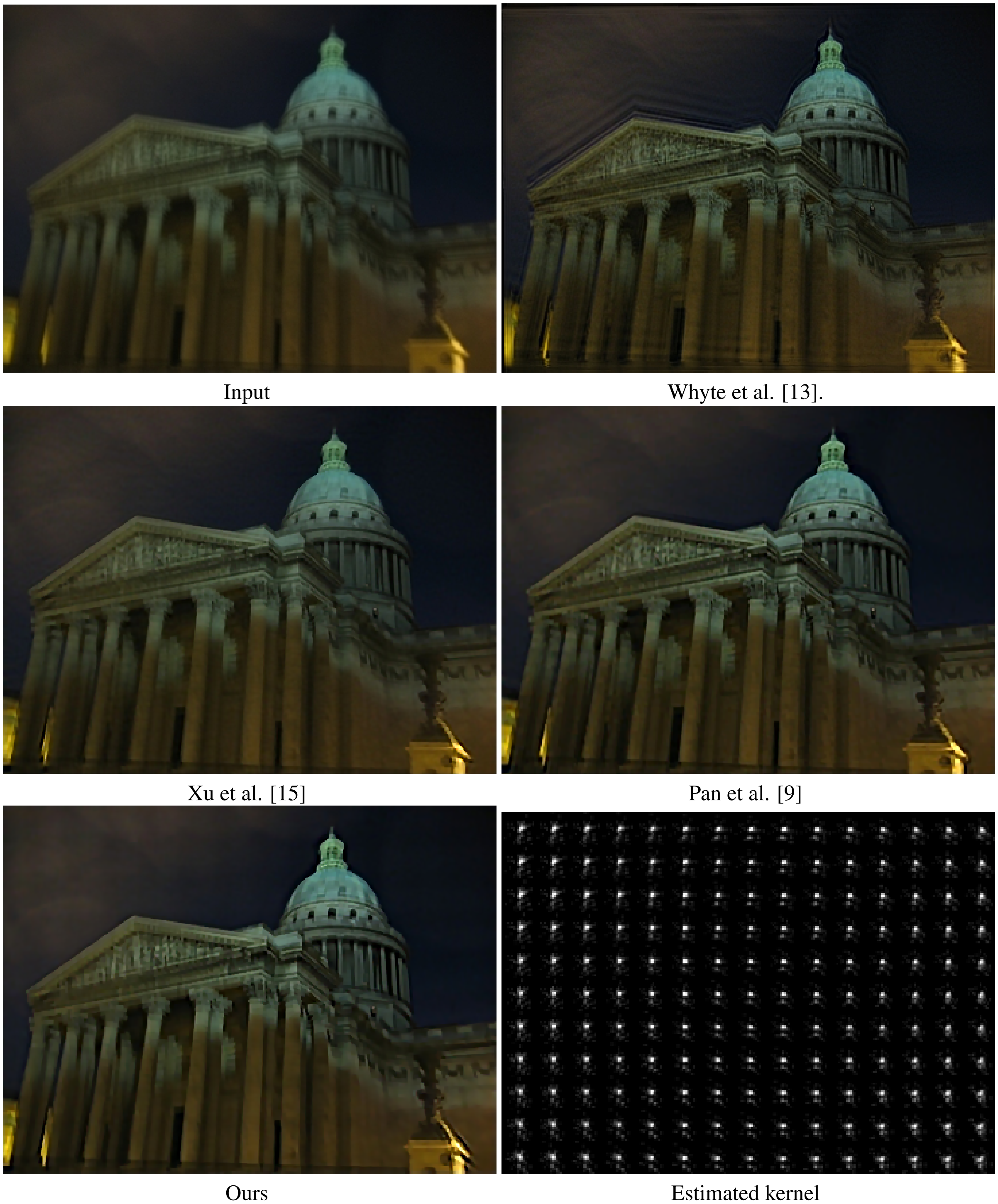

Figure 10. Deblurring non-uniform blurry image. Our method generates compareble result with state-of-the-art methods.

References

[1] Sunghyun Cho and Seungyong Lee. Fast motion deblurring. *ACM Transactions on Graphics*, 28(5):145, 2009.

[2] S. Cho, Jue Wang, and S. Lee. Handling outliers in non-blind image deconvolution. In *IEEE International Conference on Computer Vision*, pages 495–502, 2011.

[3] Robert Fergus, Barun Singh, Aaron Hertzmann, Sam T. Roweis, and William T. Freeman. Removing camera shake from a single photograph. *ACM Transactions on Graphics*, 25(3):787–794, 2006.

[4] Michael Hirsch, Christian J. Schuler, Stefan Harmeling, and Bernhard Schölkopf. Fast removal of non-uniform camera shake. In *IEEE International Conference on Computer Vision*, 2011.

[5] Zhe Hu, Sunghyun Cho, Jue Wang, and Ming-Hsuan Yang. Deblurring low-light images with light streaks. In *IEEE Conference on Computer Vision and Pattern Recognition*, pages 3382–3389, 2014.

[6] Dilip Krishnan, Terence Tay, and Rob Fergus. Blind deconvolution using a normalized sparsity measure. In *IEEE Conference on Computer Vision and Pattern Recognition*, pages 233–240, 2011.

[7] Wei-Sheng Lai, Jia-Bin Huang, Zhe Hu, Narendra Ahuja, and Ming-Hsuan Yang. A comparative study for single image blind deblurring. In *IEEE Conference on Computer Vision and Pattern Recognition*, pages 1701–1709, 2016.

[8] Jinshan Pan, Zhe Hu, Zhixun Su, and Ming-Hsuan Yang. Deblurring face images with exemplars. In *European Conference on Computer Vision*, pages 47–62, 2014.

[9] Jinshan Pan, Zhe Hu, Zhixun Su, and Ming-Hsuan Yang. l_0-regularized intensity and gradient prior for deblurring text images and beyond. *IEEE Transactions on Pattern Analysis and Machine Intelligence*, 39(2):342–355, 2017.

[10] Jinshan Pan, Deqing Sun, Hanspeter Pfister, and Ming-Hsuan Yang. Blind image deblurring using dark channel prior. In *IEEE Conference on Computer Vision and Pattern Recognition*, pages 1628–1636, 2016.

[11] Qi Shan, Jiaya Jia, and Aseem Agarwala. High-quality motion deblurring from a single image. *ACM Transactions on Graphics*, 27(3):73, 2008.

[12] Yu-Wing Tai, Ping Tan, and Michael S. Brown. Richardson-lucy deblurring for scenes under a projective motion path. *IEEE Transactions on Pattern Analysis and Machine Intelligence*, 33(8):1603–1618, 2011.

[13] Oliver Whyte, Josef Sivic, Andrew Zisserman, and Jean Ponce. Non-uniform deblurring for shaken images. *International Journal of Computer Vision*, 98(2):168–186, 2012.

[14] Li Xu and Jiaya Jia. Two-phase kernel estimation for robust motion deblurring. In *European Conference on Computer Vision*, pages 157–170, 2010.

[15] Li Xu, Shicheng Zheng, and Jiaya Jia. Unnatural l_0 sparse representation for natural image deblurring. In *IEEE Conference on Computer Vision and Pattern Recognition*, pages 1107–1114, 2013.

[16] Yanyang Yan, Wenqi Ren, Yuanfang Guo, Rui Wang, and Xiaochun Cao. Image deblurring via extreme channels prior. In *IEEE Conference on Computer Vision and Pattern Recognition*, pages 4003–4011, 2017.